Chemosphere 242 (2020) 125310

Contents lists available at ScienceDirect

Chemosphere

journal homepage: www.elsevier.com/locate/chemosphere

Impact of substrate material and chlorine/chloramine on the composition and function of a young biofilm microbial community as revealed by high-throughput 16S rRNA sequencing

Weiying Li [a, b, *], Qiaowen Tan [a, b], Wei Zhou [a, b, **], Jiping Chen [a, b], Yue Li [a, b], Feng Wang [c], Junpeng Zhang [a, b]

[a] State Key Laboratory of Pollution Control and Resource Reuse, Tongji University, Shanghai, 200092, China
[b] College of Environmental Science and Engineering, Tongji University, Shanghai, 200092, China
[c] Institute of Water Environment Technology, MCC Huatian Engineering and Technology Corporation, Nanjing, Jiangsu, 210019, China

HIGHLIGHTS

- Biomass and bacterial composition of young biofilm in drinking water was investigated.
- Paired T test proved significant change of bacterial community over time.
- *Phreatobacter* spp. was predominant in chlorinated samples.
- Cast iron showed a significant difference of microbial community from other materials.
- 16S gene based metagenomics prediction was adopted in tap water microbiome analysis.

GRAPHICAL ABSTRACT

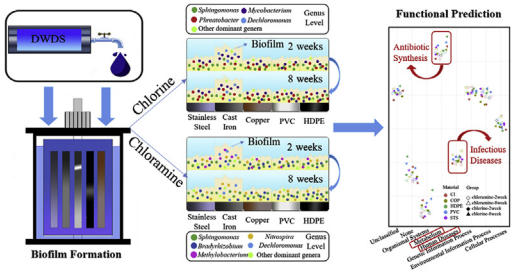

ARTICLE INFO

Article history:
Received 7 August 2019
Received in revised form
2 November 2019
Accepted 4 November 2019
Available online 5 November 2019

Handling Editor: Xiangru Zhang

Keywords:
Drinking water
Young biofilm
Disinfectant
Substrate material

ABSTRACT

The bacterial composition of biofilms in drinking water distribution systems is significantly impacted by the disinfection regime and substrate material. However, studies that have addressed the changes in the biofilm community during the early stage of formation (less than 10 weeks) were not yet adequate. Here, we explore the effects of the substrate materials (cast iron, stainless steel, copper, polyvinyl chloride, and high density polyethylene) and different disinfectants (chlorine and chloramine) on the community composition and function of young biofilm by using 16S rDNA sequencing. The results showed that *Alphaproteobacteria* (39.14%–80.87%) and *Actinobacteria* (5.90%–40.03%) were the dominant classes in chlorine-disinfection samples, while *Alphaproteobacteria* (17.46%–74.18%) and *Betaproteobacteria* (3.79%–68.50%) became dominant in a chloraminated group. The infrequently discussed genus *Phreatobacter* became predominant in the chlorinated samples, but it was inhibited by chloramine and copper ions. The key driver of the community composition was indicated as different disinfectants according to principle coordination analysis (PCoA) and Permutational multivariate analysis of variance (Adonis test), and the bacterial community changed significantly over time. Communities of biofilms grown on cast iron showed a great distance from the other materials according to Bray-Curtis dissimilarity, and they had a

* Corresponding author. State Key Laboratory of Pollution Control and Resource Reuse, Tongji University, Shanghai, 200092, China.
** Corresponding author. State Key Laboratory of Pollution Control and Resource Reuse, Tongji University, Shanghai, 200092, China.
E-mail addresses: 123lwyktz@tongji.edu.cn (W. Li), Wei_Zhou@tongji.edu.cn (W. Zhou).

https://doi.org/10.1016/j.chemosphere.2019.125310

High-throughput sequencing
Microbial community composition

unique dominant genus, *Dechloromonas*. A metagenomics prediction based on 16S rDNA was used to detect the functional pathways of antibiotic biosynthesis and beta-lactam resistance, and it revealed that several pathways were significantly different in terms of their chlorinated and chloraminated groups.

1. Introduction

The drinking water distribution system (DWDS) represent an important part of the drinking water industry. Due to the vast inner surface that contacts the bulk water in the system, the DWDS supports the growth of microorganisms and the formation of biofilms. It has been revealed that the protection provided by the extracellular polymer (EPS) in the biofilm matrix could play a critical role in the chlorine resistance of bacteria in DWDSs. In addition, DWDS biofilms may serve as a reservoir for the accumulation of opportunistic pathogens, such as *Legionella pneumophila*, nontuberculous mycobacteria (NTM) (Proctor et al., 2018), etc., which threaten immunocompromised populations.

The pipe material and disinfection strategy are two factors that have profoundly impacted the bacterial community structures in DWDSs (Jang et al., 2011; Zhu et al., 2014; Aggarwal et al., 2018). Because of the different degrees of surface roughness and the chemical activities of corrosion, the structure and formation of biofilms can vary dramatically from metal to plastic materials, but there is still controversy as to whether substrate materials have significant effects on the bacterial communities of the biofilm (Wang et al., 2014a; Aggarwal et al., 2018). In order to maintain a certain level of residual disinfectant in DWDSs and control microorganisms, chlorine (Cl_2) and chloramine (NH_2Cl) are widely used in drinking water disinfection (Jiang et al., 2017; Han and Zhang, 2018). Therefore, different disinfectants (chlorine/chloramine) could also profoundly affect the bacterial composition because compared to chlorine, chloramine has higher permeability to biofilms and lower lethality to microorganisms (Lee et al., 2011; Dodd, 2012). Moreover, the different corrosion characteristics and reaction products of chlorine/chloramine will affect the bacterial community indirectly as well. Nitrate-dependent Fe(II) oxidation reportedly proceeded greater with chloramines than with chlorine, which could favour the formation of denser corrosion scales on metal pipes (Li et al., 2015). Moreover, when chlorine was substituted with chloramines, a significant decrease in corrosion-related bacteria was observed (Wang et al., 2012b).

To date, studies have widely demonstrated the effect of the pipe material and disinfectant on mature biofilm from conducting biofilm reactors (Yu et al., 2010; Jang et al., 2011; Aggarwal et al., 2018) or sampling in real DWDSs (Henne et al., 2012; Lin et al., 2013). Relatively speaking, community composition analyses of young biofilm (less than 10 weeks old) have rarely been documented. Some studies have indicated that large variations in the biofilm structure and composition occur at the early stage of formation (Shen et al., 2016). For example, Revetta et al. (2013) analysed the net relatedness index (NRI) for biofilm communities, and they revealed a pattern of rapid increases in clustering in the community from the first to the second and third months, followed by a gradual decrease thereafter. Because the construction of high-quality drinking water facilities is being vigorously promoted in developing countries, there is important practical significance to investigating the community composition of the biofilm in its initial stage due to the replacement of municipal pipelines in DWDSs.

To fill this knowledge gap, we studied two continuously operated biofilm annular reactors to simulate the DWDSs and investigate the effects of five commonly used substrate materials, namely cast iron (CI), copper (COP), stainless steel (STS), polyvinyl chloride (PVC), high density polyethylene (HDPE), and different disinfectants (chlorine/chloramine) on the young biofilm (2 weeks and 8 weeks) community composition and function. The microbial community was determined by Illumina MiSeq high-throughput sequencing, and a functional prediction of the community was subsequently conducted. The results could promote a better understanding of the microbial community in young biofilm in DWDSs and help to ensure the biosafety of drinking water.

2. Materials and methods

2.1. Biofilm annular reactor operation

Two biofilm annular reactors (Bio Surface Technologies Co., USA) were operated continuously to simulate a practical drinking water distribution system. The rotating speed of the reactor was maintained at 50 rpm, i.e., 0.25 N/m^2, and this shear stress was equivalent to a flow of approximately 0.3 m/s in a 100-mm-diameter smooth pipe (Gomes et al., 2014). Twenty coupons containing five different materials, including CI, COP, STS, PVC, and HDPE, were installed in the two reactors. The water volume of the reactor was 1 L, and the surface area of the coupons was 17.51 cm^2 ($H \times W = 14.986\ cm \times 1.168\ cm$).

The reactors were fed by tap water in our laboratory, and the water quality was summarized in Table S1. The chlorine was prepared by diluting sodium hypochlorite solution (active chlorine > 5%, Sinopharm Chemical Reagent Co., Ltd, China) with ultrapure water (Milli-Q, USA) to a final residual chlorine concentration of 8.00 mg/L. The chloramine was prepared by mixing ammonium sulfate and sodium hypochlorite according to the mass ratio Cl:N = 4:1 and then diluted to 10.00 mg/L. The tap water and disinfectant were supplied by a peristaltic pump at flow rates of 9 mL/min and 1 mL/min, respectively. Therefore, the initial residual concentration at the inlet of the annular reactors was maintained at 0.80 mg/L for the chlorinated system and 1.00 mg/L for the chloraminated system. The concentrations of the chlorine and chloramine were determined to be an average of 0.80 mg/L when measured continuously for 45 days and an average of 1.00 mg/L when measured once a month for a year, respectively, at the outlets of two drinking water treatment plants in eastern China. The reactors were running under this condition for eight weeks. Similar bioreactor operation was reported previously by Aggarwal et al. (2018).

2.2. Sampling and DNA extraction

The biofilm samples of each material were collected during the second and eighth weeks by swabbing the coupon surfaces completely with sterile cotton, and then the swabs were placed in sterile glass bottles filled with 100 mL of phosphate buffer each. The collected biofilm samples underwent 20 min of sonication (SB-800D, Ningbo Scientz Biotechnology Co., LTD, China) in ice water to detach the biofilm from the cotton before DNA extraction. After pre-treatment, 50 mL of each biofilm mixture acquired from the

same sample was subsequently filtered through one polycarbonate membrane (0.22 μm, Millipore, USA) by vacuum pump, while the residual biofilm mixture was used for water quality analysis. The total DNA was extracted immediately using a PowerWater® DNA Isolation Kit (MOBIO, USA) according to the manufacturer's protocol.

2.3. Water quality analysis

The pH (PE20, METTLER, Switzerland), turbidity (2100Q, HACH, USA), residual chlorine (PC II, HACH, USA), and dissolved organic carbon (DOC, TOC4100, Shimadzu, Japan) were measured during this study. In addition, the assimilable organic carbon (AOC) was detected using the method introduced in our previous study (Zhang et al., 2016). Regarding the heterotrophic plate count (HPC), the samples were appropriately diluted and then plated onto R2A agar (QingDao Hope Bio-technology CO., LTD, China), and the numbers of colonies were determined after 48 h of incubation at 37 °C. The intact cell counts (ICC) were determined by flow cytometry (Prest et al., 2013). Both SYBR green and propidium iodide were added (Life Technologies Ltd., USA) for ICC detection. All the parameters were detected in triplicate.

2.4. High-throughput 16S rRNA gene sequencing

The V4–V5 region of 16S ribosomal RNA genes were amplified by PCR (95 °C for 2 min, followed by 25 cycles at 95 °C for 30 s, 55 °C for 30 s, and 72 °C for 30 s with a final extension at 72 °C for 5 min) using the primers 515F 5′-barcode-GTGCCAGCMGCCGCGG-3′ and 907R 5′-CCGTCAATTCMTTTRAGTTT-3′ (Zhang et al., 2019b), in which the barcode is an eight-base sequence unique to each sample. The PCRs were performed in triplicates of 20 μL mixtures containing 4 μL of 5 × FastPfu Buffer, 2 μL of 2.5 mM dNTPs, 0.8 μL of each primer (5 μM), 0.4 μL of FastPfu Polymerase, and 10 ng of template DNA. The amplicons were extracted from 2% agarose gels and purified using an AxyPrep DNA Gel Extraction Kit (Axygen Biosciences, Union City, CA, U.S.) according to the manufacturer's instructions and then quantified using QuantiFluor™-ST (Promega, U.S.). The purified amplicons were pooled in equimolar concentrations and paired-end sequenced (2 × 250) on an Illumina MiSeq platform according to the standard protocols.

2.5. Data analysis and functional prediction

The raw FASTQ files were demultiplexed and quality-filtered using QIIME (version 1.9.1). The 300 bp reads were truncated at any site with an average quality score <20 over a 50 bp sliding window, and truncated reads that were shorter than 50 bp were discarded. During exact barcode matching, 2-nucleotide mismatches in primer matching or reads containing ambiguous characters were removed. Only sequences with overlaps longer than 10 bp were assembled according to their 197 bp overlap sequence. Reads that could not be assembled were discarded. Operational Units (OTUs) were clustered with a 97% similarity cutoff using UPARSE (version 7.1), and chimeric sequences were identified and removed using UCHIME. The taxonomy of each 16S rRNA gene sequence was analysed by RDP Classifier (http://rdp.cme.msu.edu/) against the SILVA (SSU 123) 16S rRNA database using a confidence threshold of 70%. The representative sequences of pathogen-like OTUs were compared with the NCBI Bacteria and Archaea database by BLASTN tool (Wang et al., 2014a).

Bray-Curtis dissimilarities are based on individual OTUs, and they were computed for the principal coordinates analyses (PCoA) and hierarchical clustering using "vegan" and "ape" R packages and plotted by the "ggplot2" package. Random Forest-supervised learning models (mtry = 20 and ntree = 800) were used to identify the important genera by calculating the mean decrease accuracy and Gini index in the "randomForest" R package (Abia et al., 2019). Permutational multivariate analysis of variance (Adonis test) (999 permutations) were conducted using the adonis2 function in the "vegan" R package to analyse the significance of the community differences. Paired-sample Student's t-tests were conducted using SPSS to test the properties with significant differences among the groups. The functional gene prediction of the biofilm bacterial community was assessed using PICRUSt (version 0.9.1) on Galaxy (Langille et al., 2013).

3. Results and dissuasion

3.1. Physicochemical and biomass properties of the biofilm mixture and water

The Cu^{2+} concentration, organic properties in terms of DOC and AOC, and biomass properties in terms of the HPC and ICC of the biofilm mixture were tested in this study. In addition, the water quality of the inlet and outlet water from the chlorinated and chloraminated reactors was monitored for free chlorine/total chlorine, turbidity and DOC (Table S1).

Regarding the organic carbon properties in the biofilm mixture, the DOC was observed to be higher in biofilms grown on plastic materials than others grown in the chlorinated group, but there was no similar phenomenon in the chloraminated ones. The AOC/DOC, which characterizes the proportion of carbon that can be assimilated by bacteria to total organic carbon, was highest in the biofilm on cast iron among all the samples. However, the AOC/DOC showed no obvious regularities in the other materials (Table 1 and Table 2). The HPC and ICC were tested to characterize the cultivable heterotrophic bacteria and bacteria with intact membranes in the biofilm, respectively. The results revealed that both properties were dramatically higher in the cast iron coupons than they were for the other biofilms, which indicated that the biofilm grown on cast iron had the highest biomass among the five materials. In addition, relatively low HPC and ICC values and a high concentration of copper ions were observed in the biofilms on copper coupons (Tables 1 and 2). The HPC/ICC was calculated to reflect the proportion of cultivable heterotrophic bacteria among the total bacteria to some extent. The results showed that the ratio varied from 1.38% to 5.61%, and it was higher in the chlorinated group than in the chloraminated group (except for the 8-week copper biofilm) (Tables 1 and 2).

According to the results, the highest and lowest levels of biomass were found in cast iron and copper-grown biofilms for both growth times and for both chlorine/chloramine, respectively. Previous studies have shown that bacteria could easily accumulate in iron pipes (Jang et al., 2011; Ren et al., 2015). The CI coupon had higher surface roughness than the other coupon materials in our study, which was one prominent advantage for bacterial colonization. In addition, due to the relatively higher chemical reactivity of Fe, iron reacted easily with chlorine/chloramine, resulting in the corrosion of these pipes. Corrosive holes could provide ideal habitants for protecting bacteria from adverse environments, such as residual chlorine, etc. The high concentration of AOC and the high ratio of AOC/DOC also represented a necessary factor for the high biomass on the cast iron material. By contrast, the smooth surface and the stable chemical properties of copper and stainless steel caused a lower biofilm biomass. These results indicated that the Cu^{2+} was released from the copper material and accumulated in the biofilm, and it was toxic to the microorganisms, leading to a lower bacterial quantity.

Regarding the plastic materials, studies have demonstrated that

Table 1
Water quantities of biofilm mixture acquired from chlorinated samples.

Sample ID		DOC (mg/L)	AOC (mg/L)	AOC/DOC	HPC (CFU/cm^2)	ICC (cells/cm^2)	HPC/ICC	Cu (μg/L)
Two weeks	PVC	2.31 ± 0.15	0.69 ± 0.02	29.87%	$6.41 \pm 0.28 \times 10^4$	$1.14 \pm 0.00 \times 10^6$	5.61%	14.95
	HDPE	2.39 ± 0.08	0.76 ± 0.06	31.80%	$8.56 \pm 0.26 \times 10^4$	$1.53 \pm 0.14 \times 10^6$	5.59%	15.39
	CI	2.39 ± 0.08	0.94 ± 0.10	43.12%	$2.77 \pm 0.29 \times 10^5$	$6.52 \pm 0.16 \times 10^6$	4.25%	43.19
	COP	2.18 ± 0.20	0.74 ± 0.03	40.66%	$1.86 \pm 0.19 \times 10^4$	$4.99 \pm 0.05 \times 10^5$	3.72%	64.49
	STS	1.95 ± 0.16	0.32 ± 0.08	16.41%	$3.54 \pm 0.16 \times 10^4$	$1.08 \pm 0.01 \times 10^6$	3.30%	18.08
Eight weeks	PVC	2.50 ± 0.10	1.16 ± 0.11	46.42%	$5.95 \pm 0.22 \times 10^4$	$1.55 \pm 0.01 \times 10^6$	3.84%	21.05
	HDPE	2.38 ± 0.24	0.79 ± 0.03	33.07%	$6.77 \pm 0.21 \times 10^4$	$1.73 \pm 0.01 \times 10^6$	3.90%	12.25
	CI	1.58 ± 0.24	0.90 ± 0.02	56.96%	$1.22 \pm 0.07 \times 10^5$	$2.91 \pm 0.01 \times 10^6$	4.18%	21.08
	COP	1.68 ± 0.17	0.49 ± 0.02	29.87%	$1.35 \pm 0.15 \times 10^4$	$9.76 \pm 0.09 \times 10^5$	1.38%	28.53
	STS	1.18 ± 0.38	0.47 ± 0.02	40.03%	$6.4 \pm 0.26 \times 10^4$	$1.73 \pm 0.04 \times 10^6$	3.70%	24.15

Table 2
Water quantities of biofilm mixture acquired from chloraminated samples.

Sample ID		DOC (mg/L)	AOC (mg/L)	AOC/DOC	HPC (CFU/cm^2)	ICC (cells/cm^2)	HPC/ICC	Cu (μg/L)
Two weeks	PVC	1.31 ± 0.14	0.37 ± 0.02	28.04%	$2.85 \pm 0.20 \times 10^4$	$1.34 \pm 0.02 \times 10^6$	2.14%	9.44
	HDPE	2.23 ± 0.11	0.49 ± 0.03	21.78%	$2.08 \pm 0.28 \times 10^4$	$1.00 \pm 0.01 \times 10^6$	2.08%	17.57
	CI	2.70 ± 0.15	0.97 ± 0.09	35.88%	$2.06 \pm 0.19 \times 10^5$	$7.20 \pm 0.02 \times 10^6$	2.87%	29.94
	COP	2.64 ± 0.11	0.41 ± 0.03	15.43%	$1.76 \pm 0.19 \times 10^4$	$1.32 \pm 0.00 \times 10^6$	1.33%	73.79
	STS	1.40 ± 0.08	0.47 ± 0.07	33.81%	$2.51 \pm 0.19 \times 10^4$	$1.04 \pm 0.01 \times 10^6$	2.42%	3.85
Eight weeks	PVC	1.71 ± 0.08	0.44 ± 0.09	25.83%	$2.43 \pm 0.11 \times 10^4$	$1.84 \pm 0.01 \times 10^6$	1.32%	12.11
	HDPE	2.32 ± 0.16	0.57 ± 0.04	24.53%	$3.33 \pm 0.14 \times 10^4$	$2.56 \pm 0.00 \times 10^6$	1.30%	12.16
	CI	2.78 ± 0.34	0.76 ± 0.1	27.27%	$1.81 \pm 0.07 \times 10^5$	$7.34 \pm 0.01 \times 10^6$	2.44%	9.20
	COP	2.20 ± 0.13	0.48 ± 0.07	21.65%	$2.31 \pm 0.14 \times 10^4$	$1.56 \pm 0.00 \times 10^6$	1.48%	25.08
	STS	2.16 ± 0.27	0.44 ± 0.04	20.42%	$2.54 \pm 0.25 \times 10^4$	$1.13 \pm 0.04 \times 10^6$	2.25%	3.88

the unexpected migration of organic compounds always occurred in the presence of an oxidant (Adams et al., 2011). This migration caused a higher concentration of organic carbon in biofilm grown on PVC and HDPE, which may facilitate the bacterial growth to some extent. Moreover, the ratio of HPC and ICC was found to be lower in the chloraminated samples compared to the chlorinated samples. The accumulation and domination of the nitrifying bacteria (a type of autotrophic bacteria) *Nitrosomonas* spp. and *Nitrospira* spp. due to the presence of chloramine may explain this phenomenon to some extent.

3.2. Bacterial community diversity and richness

The species richness estimators by Chao and Ace and the species diversity indexes by Shannon and Simpson were adapted to analyse the biodiversity in this study.

Regarding the chlorinated samples, the Chao and Ace indexes clearly showed that the community richness of two-week-old biofilms was higher than that of eight-week-old biofilms for each material. However, a higher Shannon index of 8-week biofilms (except for STS) compared to 2-week biofilms indicated that the community evenness of the 8-week biofilms was higher (Table S2). A similar result was also obtained by calculating the Shannoneven index (Table S4). The Shannon index also revealed that the community diversity of the biofilm collected from plastic materials (HDPE and PVC) was the lowest in both the 2-week and 8-week groups. Additionally, the diversity and richness were much higher in the two-week STS biofilm (Table S2).

Compared to chlorine disinfection, the OTU number and the Chao and Ace indexes clearly showed that the community richness of the chloraminated samples was lower, except for the 8-week STS and HDPE biofilms. However, the Simpson and Shannon results revealed that the community diversity was higher in the chloraminated system, unlike the 2-week STS (Table S3), which indicated that there were fewer species of bacteria growing on the biofilm in the chloraminated system, but they could proliferate more evenly, which was also confirmed by the Shannoneven index (Table S4). The Shannon index also showed an increase in the community diversity over time (except for PVC). The highest community diversity was found in the PVC and CI biofilms in the 2-week and 8-week groups, respectively (Table S3).

3.3. Biofilm bacterial community composition

3.3.1. Dominant classes and genera

The dominant class and genus in each biofilm sample from the chlorine and chloramine disinfection groups were demonstrated by bar plot in Fig. 1 and Fig. S1. At the class level, *Alphaproteobacteria* (39.14%–80.87%) and *Actinobacteria* (5.90%–40.03%) were dominant in all the chlorine-disinfection samples, and *Betaproteobacteria* was found to be relatively high only in the biofilm from CI material (21.59% and 26.46% in 2-week and 8-week samples, respectively) compared to the others. Regarding the chloraminated samples, *Alphaproteobacteria* (17.46%–74.18%) and *Betaproteobacteria* (3.79%–68.50%) were the two dominant classes.

At the genus level, *Sphingomonas* (17.75%–53.76%) and *Mycobacterium* (5.08%–39.12%) were dominant in all the chlorine-disinfection samples, while *Phreatobacter* (7.29%–43.00%) was another dominant component. However, an interesting phenomenon was that COP material has an inhibiting effect on this genus (Fig. S1). In the chloraminated group, *Sphingomonas* (1.11%–30.74%) was also dominant but showed a relatively lower abundance compared to the chlorinated samples. Additionally, *Bradyrhizobium*, *Methylobacterium*, *Nitrospira*, etc. became abundant in the chloraminated system (Fig. S1). In addition, the abundance of *Dechloromonas* was indicated to be relatively high in all the CI samples, regardless of the disinfection strategy.

Random forest classification is a widely-used machine learning algorithm, which can be applied in the study of microbiology to identify important variables between experimental groups (Abia et al., 2019). In the current study, the top 40 dominant genera in all the samples were selected to train the random forest model. The mean decrease in accuracy and Gini value were two reliable and relevant predictors for performing classifications, which were used

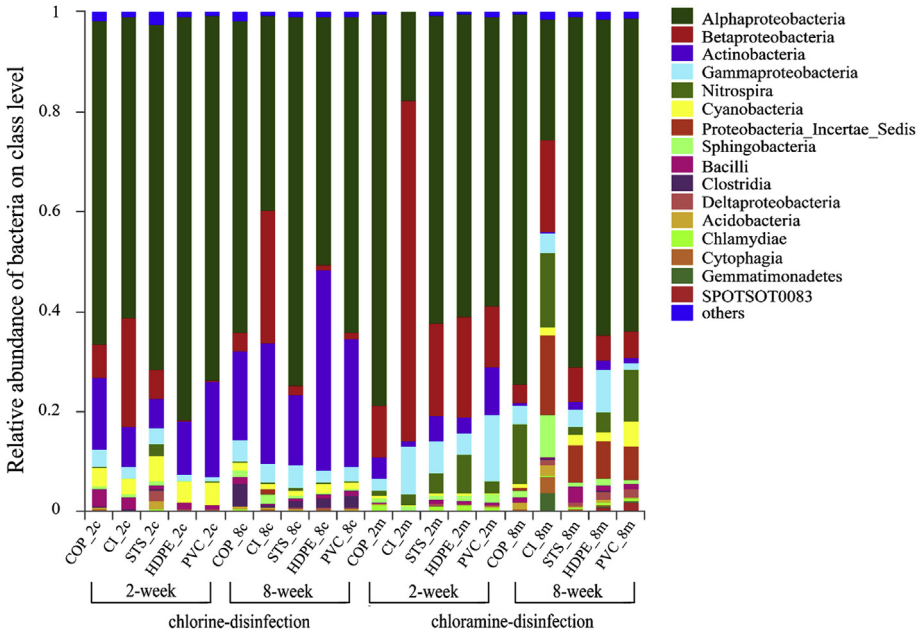

Fig. 1. Bacterial community profiles of biofilm samples at the class level. (Sample designation: "2" refers to "two-week", "8" refers to "eight-week", "c" refers to "chlorine disinfection", and "m" refers to "chloramine disinfection").

to identify the most essential genera between the chlorinated and chloraminated groups. Higher values in both the decrease of accuracy and of the Gini value represent the higher importance of a genus (Fig. 2).

The use of different disinfection strategies was considered to be a crucial factor that shaped the DWDS microbiome profoundly, whether in biofilm or bulk water samples (Gomez-Alvarez et al., 2012; Hwang et al., 2012; Wang et al., 2012a; Zhang et al., 2019a). Chlorine/chloramine could impact the biofilm microorganisms differently because chloramine could penetrate the biofilm more strongly, while chlorine could better inactivate the microorganisms near the biofilm surface with a stronger oxidant reactivity (Lee et al., 2011; Dodd, 2012). Apart from these reasons, the chemical components of disinfectants may be involved in the metabolisms of some bacteria, and the corrosion of the pipe wall would also affect the microbiome. At the class level, Wang et al. (2014a) reported that *Alphaproteobacteria*, *Betaproteobacteria* and *Bacteroidetes* were dominant in both chlorinated and chloraminated simulated distribution systems (SDSs), while the chloraminated system possessed a higher abundance of *Alphaproteobacteria*, which was consistent with our study to some extent. The infrequently documented genus *Phreatobacter* was predominant in the chlorinated

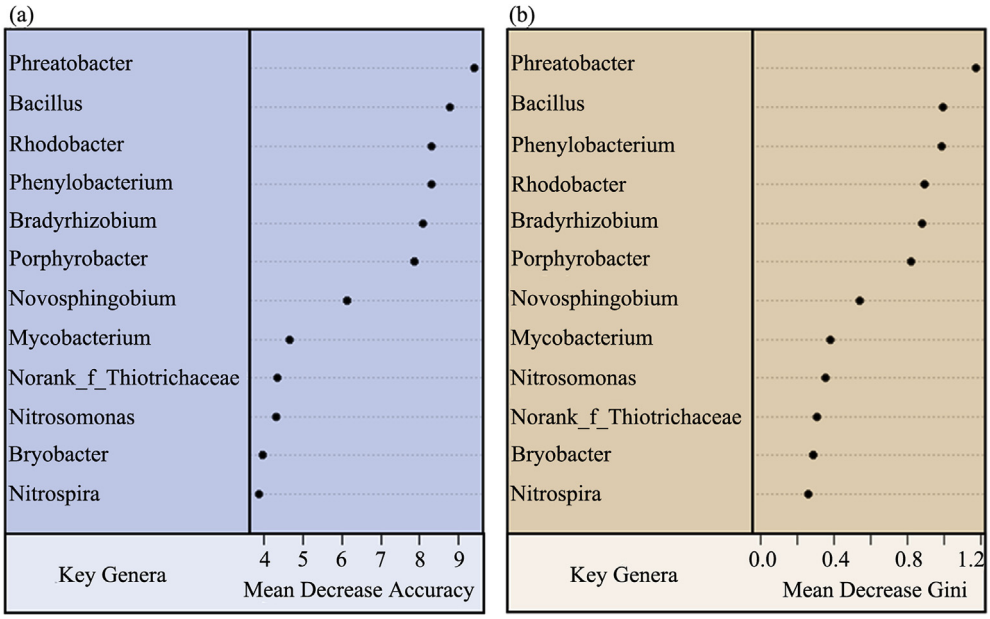

Fig. 2. Two indexes, namely, the (a) mean decrease in accuracy and (b) mean decrease in Gini, were calculated with a trained "random forest" model, which revealed the essential genera that triggered the difference between the chlorinated and chloraminated groups.

samples. However, a recent article reported its dominance in drinking water in the DWDSs of Paris (Perrin et al., 2019), and it tended to be more abundant in water with low chlorine concentrations (Stanish et al., 2016). Our study implied that the abundance of *Phreatobacter* in the planktonic microbial population could result from biofilm, and it can be sensitive to chloramine disinfection and the accumulation of Cu^{2+}. As reported before, *Dechloromonas* spp. exhibited stronger corrosion inhibition by inducing the redox cycling of iron to enhance the precipitation of iron oxides and the formation of Fe_3O_4, and it became dominant (40.08%) after 20 days of growth on cast iron (Wang et al., 2014b). The dominance of *Dechloromonas* spp. in this study could be a sign of the formation of a combat corrosion layer on the cast iron.

3.3.2. Potential pathogens

In order to obtain the information about the profiles of pathogenic colonization in the biofilm samples, a total of 23 OTUs in all the samples annotated as *Mycobacterium* spp., *Legionella* spp., *S. paucimobilis*, *S. aureus* and *P. aeruginosa* were selected and subjected to a BLAST search against the NCBI Bacteria and Archaea database (Table S5). *Mycobacterium* was observed to be a dominant genus in the chlorinated biofilms, and there was an obvious difference in the relative abundance between the chlorinated and chloraminated groups ($p < 0.001$, paired-sample *t*-test). There were five OTUs that were classified as *Mycobacterium* spp., and the best BLAST hit of the representative sequences revealed the closest matches were with *M. mucogenicum*, *M. gadium*, *M, paragordonae*, *M. shigaense* and *M. kyorinense*. OTU49 showed relatively high similarity with *M. intracellulare* strain ATCC 13950 and *M. avium* strain ATCC 25291 (score = 789, ident = 98.87%, and 100% query cover), which belonged to nontuberculous mycobacteria (NTM). Sixteen OTUs were identified as *Legionella* spp., among which OTU424 was closely related to *L. pneumophila* (score = 754, ident = 97%, 100% query cover). OTU1017 and OTU1019 showed the highest similarity to *P. aeruginosa* and *S. paucimobilis*, respectively. Additionally, the representative sequence analysis revealed that OTU1012 was highly similar to *S. aureus* (score = 804, ident = 99%, 100% query cover).

Opportunistic pathogens such as *Mycobacterium* spp., *Legionella* spp., *S. paucimobilis*, *P. aeruginosa* and *S. aureus* in drinking water are of great public health concern because they pose potential infectious threats to immunocompromised populations. *Mycobacterium* spp. is widely accepted to be a highly chlorine-resistant bacterium. Unlike the current research result, *Mycobacterium* spp. was previously reported to be dominant in biofilm and bulk water treated with chloramine disinfection (Beumer et al., 2010; Revetta et al., 2013). Revetta et al. (2013) conducted an 8-month biofilm test in monochloramine-treated drinking water, and the results showed that *Mycobacterium*-like phylotypes became the most predominant populations (>27%) during subsequent months, but not during the early stages of biofilm formation. This finding may explain why the young biofilm in the chloraminated system displayed no *Mycobacterium* enrichment.

3.4. Key factors account for the difference in the bacterial community composition

Hierarchical clustering and principal PCoA on the OTU level were employed to test the key factors that drive the variation in the community composition. These analyses clearly clustered all the samples into two groups according to the chlorine/chloramine disinfection (Fig. 3a and Fig. 4). Within each disinfectant group, they also demonstrated a tendency in the samples to accumulate according to the growth time of the biofilm (Fig. 3b and c, and Fig. 4). Adonis/PERMANOVA tests were subsequently conducted and the results revealed that the community compositions of the four groups (chlorine/chloramine × 2-weeks/8-weeks) were significantly different ($R^2 = 0.57$, $p = 0.001$). A pairwise comparison supported the homogeneity of dispersion between the four groups and between each of the two groups (Table S6), which supports the results of the PCoA. A two-way Adonis test was conducted across all the coupon materials to test the overall and marginal effects of the disinfectant and growth time on the biofilm community composition, and it revealed that different disinfectants had more significant effects on the positions of samples in the multivariate space (Table S7). The results of a paired-sample *t*-test regarding the coordination on PC1 and PC2 further confirmed the results of Adonis test and the significant impact of the grouping factors (Tables S8 and S9).

Within each group, the PCoA and hierarchical analysis revealed different clustering characteristics according to the coupon materials. In the chlorinated group, samples from STS, HDPE and PVC showed a tendency to gather according to the growth time, and samples from CI and COP were far away from them. Regarding the chloraminated group, samples from CI were also clearly separated from the STS, HDPE, PVC and COP clusters in their respective growth time groups.

To date, changes in the microbiome during the early stages of biofilm development have not been explored sufficiently and thoroughly. The DWDS biofilms were suggested to reach a steady state within one to three years (Martiny et al., 2003). Before this period, the shift in the bacterial community of the biofilm could be dramatic. In the current study, both the PCoA plot and the statistical analysis indicated that the biofilm bacterial community shifted significantly over time. In the chlorinated group, if COP and CI biofilms were excluded, other chlorinated samples were separated according to the growth time, as suggested by the community bar plot and PCoA (Figs. 1 and 2 and Fig. S1). In addition, the results of Beta-diversity also yield novel information compared to previous study. Aggarwal et al. (2018) demonstrated the change in the biofilm community over a relatively long time. The results showed that the 15-month (set B) and 28-month biofilms (set C) were more similar according to the composition of the bacteria compared to the 13-month biofilms (set A). However, the significant heterogeneity of dispersion confounded the Adonis results, whereas the equivalent dispersion between groups in this study confirmed the validity of time factor as a key driver of bacterial community composition.

It was previously shown that the roughness of the substrate surface and the corrosion products would affect the bacterial attachment. This finding was confirmed here in that the Bray-Curtis distance of the CI biofilms was far from the others while the STS, PVC and HDPE biofilms were clustered in each group (Fig. 3). In addition, the Shannon index indicated that the biodiversity on the CI material increased in the 8-week samples and became the highest, which was consistent with previous studies (Lin et al., 2013; Wang et al., 2014a; Zhu et al., 2014). The high roughness and surface area were favourable for biofilm attachment and suitable for more microorganism species to survive and proliferate (Yu et al., 2010), which was supported by the HPC and ICC results as well.

3.5. Functional profiles of the biofilm bacterial community

The overall functional profiles of the bacterial communities in the biofilm samples were obtained based on OTU information using PICRUSt (online methods) (Fig. 5). The nearest sequenced taxon index (NSTI) of the 20 samples were 0.07 ± 0.02, which revealed the accuracy of each prediction by calculating the sum of the phylogenetic distances for each organism in the OTU table to its nearest

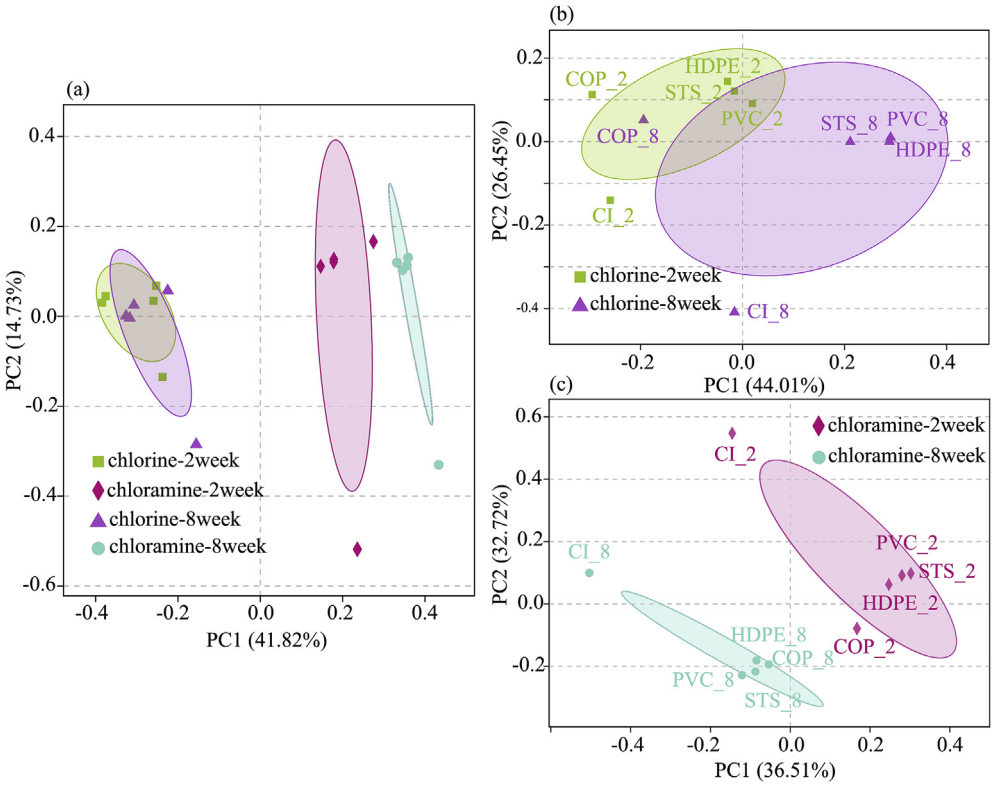

Fig. 3. PCoA plots based on Bray-Curtis dissimilarities showing the clustering of the bacterial community compositions for (a) all the samples, (b) chlorinated biofilm samples, and (c) chloraminated biofilm samples.

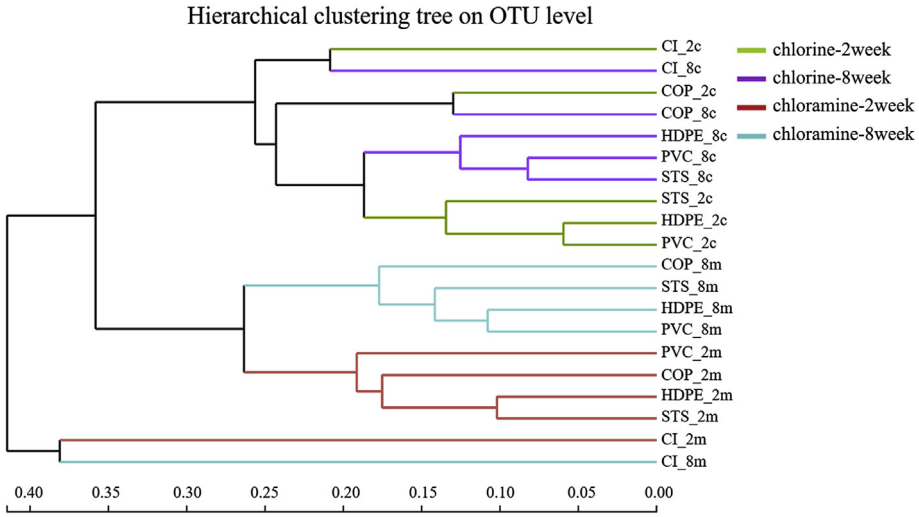

Fig. 4. Hierarchical clustering plot based on the Bray-Curtis dissimilarities showing the clustering of the bacterial community compositions for all the samples.

relative with a reference genome. A total of 329 KEGG pathways were classified, and they belonged to seven level 1 categories including cellular processes, environmental information processing, genetic information processing, human diseases, metabolism, organismal systems and unclassified, with involvement in metabolic activities being the most recorded, followed by the pathways relating to genetic and environmental information processing (Fig. 5).

Six level 2 classes belonging to human diseases were identified, including cancers, cardiovascular diseases, immune system diseases, infectious diseases, metabolic diseases and neurodegenerative diseases, with infectious diseases being the most abundant function. Fig. 6a shows the heat map of the top 10 abundant sub-level functions pertaining to infectious diseases. A paired Student's t-test revealed that the pathways for pertussis ($p < 0.05$), the *Vibrio cholera* pathogenic cycle ($p < 0.01$), and tuberculosis ($p < 0.05$) were significantly more abundant in the chloraminated samples than in the chlorinated samples. Inversely, pathways for African trypanosomiasis ($p < 0.01$) and Chagas disease (American trypanosomiasis) ($p < 0.05$) were verified to be more abundant in

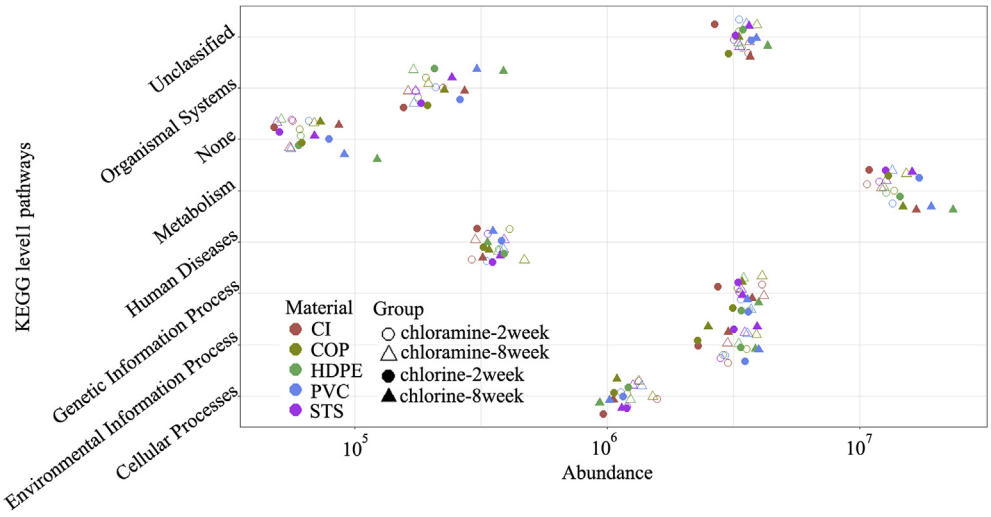

Fig. 5. Abundance of KEGG pathway groups (level 1) in each biofilm bacterial community by 16S-based functional prediction.

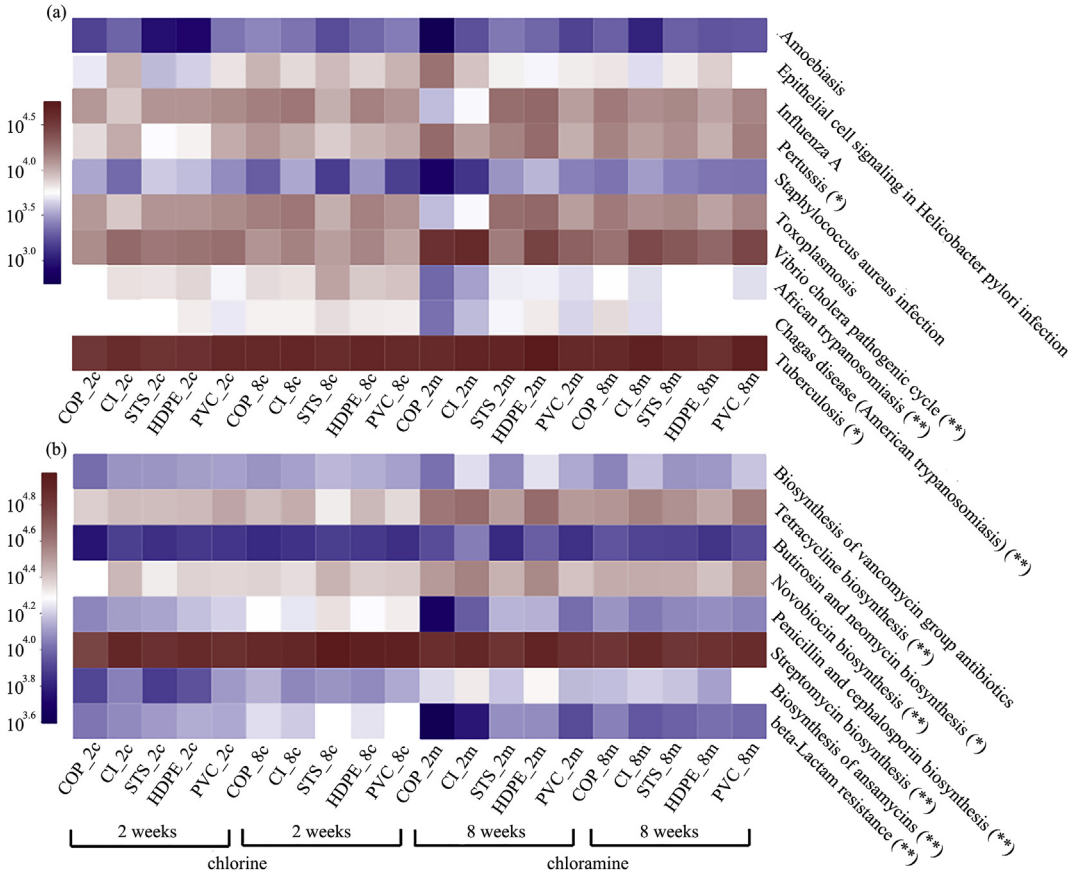

Fig. 6. Heat map of KEGG pathways for the abundance of (a) human disease and (b) antibiotic related biosynthesis (* and ** refer to significant difference between chlorinated and chloraminated groups: $^*p < 0.05$, $^{**}p < 0.01$).

the chlorinated samples.

The abundance of antibiotic biosynthesis-associated pathways, including those for vancomycin, tetracycline, butirosin and neomycin, novobiocin, penicillin and cephalosporin, streptomycin, and ansamycins and one antibiotic resistance-associated pathway, for beta-lactam resistance, were demonstrated by heat map (Fig. 6b). The pathways for tetracycline biosynthesis ($p < 0.01$), butirosin and neomycin biosynthesis ($p < 0.05$), bovobiocin biosynthesis ($p < 0.01$), and ansamycin biosynthesis ($p < 0.01$) were significantly higher in the chloramine-treated biofilms. The penicillin and cephalosporin biosynthesis ($p < 0.01$) and the beta-lactam resistance ($p < 0.01$) were significantly higher in chlorine-treated biofilms.

Metagenomic predictions based on 16S rRNA sequencing have

been widely used for describing the microbial community function in environmental research (Langille et al., 2013; Wang et al., 2018). Here, this method was introduced to investigate the profile of the biofilm bacterial function in drinking water to a comprehensive extent. The NSTI results showed that the PICRUSt analysis was accurate. According to Langille et al. (2013), the NSTI values of the biofilm samples here were slighter higher than the human gut samples but they outperformed soil samples, indicating that PICRUSt is a promising technology for drinking water microbiome analyses.

The functional prediction revealed that a considerable proportion of the microbial community in the biofilm samples was linked to human diseases (Fig. 5), and the infectious disease-related KEGG pathway was the most frequently detected in this category, which suggested that the DWDS biofilms could be an incubator of bacteria causing infectious diseases. Waterborne infection-related gene functions were detected, and, in particular, the abundant presence of *Staphylococcus aureus* infection and tuberculosis pathways may be attributed to the presence of *S. aureus*-like OTU1012 and the dominant genus *Mycobacterium*. Although culture-independent technology-16s rRNA sequencing cannot identify whether these genes were possessed by viable species, the potential risk of infectious diseases was still present due to gene communication among bacteria, such as horizontal gene transfer (Salyers and Shoemaker, 2006; Jutkina et al., 2016) or the uptake of free DNA in the biofilm environment.

Antibiotic resistance genes (ARGs) in the pathway for beta-lactam resistance were detected (Fig. 6b). The beta-lactam derivatives include penicillins, cephalosporins, etc., which have important antibacterial activities through the inhibition of bacterial cell wall biosynthesis (Hosseyni and Jarrahpour, 2018). However, due to the biosynthesis of beta-lactamase by antibiotic-resistant bacteria (ARB), these antibiotics can be deactivated (Allen et al., 2010). The presence of ARGs, including the beta-lactam resistance gene, was previously found in DWDSs (Xu et al., 2016) and tap water (Ma et al., 2017) by high throughput qPCR and metagenomics sequencing, which were consistent with the 16S rDNA functional prediction here. In particular, due to the high cell density and matrix protection of DWDS biofilms (Balcazar et al., 2015), ARGs could be enriched and transferred by gene communication, subsequently leading to an increase of ARB in the drinking water from biofilm detachment (Zhang et al., 2018). In a previous study by our group, the presence of sulfamethoxazole-, clindamycin-, and norfloxacin-resistant bacteria was investigated in DWDS biofilm (Zhang et al., 2018), and the detection of beta-lactam resistance here could be a supplemental piece of information.

In addition, several antibiotic biosynthesis-related pathways were found, indicating that the DWDS biofilms may harbour antibiotic-producing bacteria, which presents the potential to exert selective pressure and thus contaminate drinking water as well as induce the emergence and spread of bacterial resistance. Zhang et al. (2019c) investigated the long-term impact of norfloxacin and erythromycin in trace concentrations (1 μg/L) on an Anammox biofilm, and they found that erythromycin induced the amplification of the two ARGs *ermB* and *mph*. The academic community believed that antibiotics and antibiotic resistance in tap water were associated with antibiotic residues in the aquatic environment but neglected the biosynthesis of colonized bacteria in DWDS biofilms. The results of these functional profiles may provide a new direction for future research on the interaction of antibiotic biosynthesis and antibiotic resistance as well as investigations about the bio-safety issues that may arise from antibiotic-producing bacteria in drinking water biofilms.

4. Conclusion

The current study investigated the micro-ecology of young biofilms in drinking water and the relevant factors that cause changes in bacterial community composition. The type of disinfectant added was the most important factor triggered the switch of bacterial composition while a significant difference of bacterial community was also observed between 2-week and 8-week groups. Cast iron may serve as an ideal substrate supporting high biomass and bio-diversity, and the biofilms on it showed a significant difference of community composition from other materials while samples from STS, HDPE and PVC showed a tendency to gather within each group. The dominance of *Dechloromonas* spp. indicated the occurrence of corrosion inhibition and the formation of compact corrosion layer on cast iron. Metagenomics function prediction revealed that infectious diseases functional profiles were involved in *S. aureus* infections and tuberculosis, etc. Signatures related to beta-Lactam resistance and in the synthesis of potent antibiotics were also identified. This study suggests that there could be a drastic variation of bacterial composition and the occurrence of pathogenic colonization in biofilms during early stage of formation. Further investigations by metagenomics are required to evaluate the effect of biosynthesis of potent antibiotics on the fate of antibiotic resistance in DWDS biofilms.

Acknowledgements

We are grateful for the cooperation and participation of the utilities that were involved, which are supported by Natural Science Foundation of China (Project No. 51979194), China's National Critical Project for Science and Technology on Water Pollution Prevention and Control (Project No. 2017ZX07201001), the Major project of ChengDu ChuanLi intelligence fluid equipment Co., Ltd. (Project No. 20182078), and the Major project of WPG (Shanghai) Smart Water Public Co., Ltd. (Project No. 20183231).

Appendix A. Supplementary data

Supplementary data to this article can be found online at https://doi.org/10.1016/j.chemosphere.2019.125310.

References

Abia, A.L.K., Alisoltani, A., Ubomba-Jaswa, E., Dippenaar, M.A., 2019. Microbial life beyond the grave: 16S rRNA gene-based metagenomic analysis of bacteria diversity and their functional profiles in cemetery environments. Sci. Total Environ. 655, 831–841.

Adams, W.A., Xu, Y., Little, J.C., Fristachi, A.F., Rice, G.E., Impellitteri, C.A., 2011. Predicting the migration rate of dialkyl organotins from PVC pipe into water. Environ. Sci. Technol. 45, 6902–6907.

Aggarwal, S., Gomez-Smith, C.K., Jeon, Y., LaPara, T.M., Waak, M.B., Hozalski, R.M., 2018. Effects of chloramine and coupon material on biofilm abundance and community composition in bench-scale simulated water distribution systems and comparison with full-scale water mains. Environ. Sci. Technol. 52, 13077–13088.

Allen, H.K., Donato, J., Wang, H.H., Cloud-Hansen, K.A., Davies, J., Handelsman, J., 2010. Call of the wild: antibiotic resistance genes in natural environments. Nat. Rev. Microbiol. 8, 251–259.

Balcazar, J.L., Subirats, J., Borrego, C.M., 2015. The role of biofilms as environmental reservoirs of antibiotic resistance. Front. Microbiol. 6.

Beumer, A., King, D., Donohue, M., Mistry, J., Covert, T., Pfaller, S., 2010. Detection of Mycobacterium avium subsp. paratuberculosis in drinking water and biofilms by quantitative PCR. Appl. Environ. Microbiol. 76, 7367–7370.

Dodd, M.C., 2012. Potential impacts of disinfection processes on elimination and deactivation of antibiotic resistance genes during water and wastewater treatment. J. Environ. Monit. 14, 1754–1771.

Gomes, I.B., Simoes, M., Simoes, L.C., 2014. An overview on the reactors to study drinking water biofilms. Water Res. 62, 63–87.

Gomez-Alvarez, V., Revetta, R.P., Domingo, J.W.S., 2012. Metagenomic analyses of drinking water receiving different disinfection treatments. Appl. Environ. Microbiol. 78, 6095–6102.

Han, J.R., Zhang, X.R., 2018. Evaluating the comparative toxicity of DBP mixtures from different disinfection scenarios: a new approach by combining freeze drying or rotoevaporation with a marine polychaete bioassay. Environ. Sci. Technol. 52, 10552–10561.
Henne, K., Kahlisch, L., Brettar, I., Hofle, M.G., 2012. Analysis of structure and composition of bacterial core communities in mature drinking water biofilms and bulk water of a citywide network in Germany. Appl. Environ. Microbiol. 78, 3530–3538.
Hosseyni, S., Jarrahpour, A., 2018. Recent advances in beta-lactam synthesis. Org. Biomol. Chem. 16, 6840–6852.
Hwang, C., Ling, F.Q., Andersen, G.L., LeChevallier, M.W., Liu, W.T., 2012. Microbial community dynamics of an urban drinking water distribution system subjected to phases of chloramination and chlorination treatments. Appl. Environ. Microbiol. 78, 7856–7865.
Jang, H.J., Choi, Y.J., Ka, J.O., 2011. Effects of diverse water pipe materials on bacterial communities and water quality in the annular reactor. J. Microbiol. Biotechnol. 21, 115–123.
Jiang, J.Y., Zhang, X.R., Zhu, X.H., Li, Y., 2017. Removal of intermediate aromatic halogenated DBPs by activated carbon adsorption: a new approach to controlling halogenated DBPs in chlorinated drinking water. Environ. Sci. Technol. 51, 3435–3444.
Jutkina, J., Rutgersson, C., Flach, C.F., Larsson, D.G.J., 2016. An assay for determining minimal concentrations of antibiotics that drive horizontal transfer of resistance. Sci. Total Environ. 548, 131–138.
Langille, M.G.I., Zaneveld, J., Caporaso, J.G., McDonald, D., Knights, D., Reyes, J.A., Clemente, J.C., Burkepile, D.E., Thurber, R.L.V., Knight, R., Beiko, R.G., Huttenhower, C., 2013. Predictive functional profiling of microbial communities using 16S rRNA marker gene sequences. Nat. Biotechnol. 31, 814–821.
Lee, W.H., Wahman, D.G., Bishop, P.L., Pressman, J.G., 2011. Free chlorine and monochloramine application to nitrifying biofilm: comparison of biofilm penetration, activity, and viability. Environ. Sci. Technol. 45, 1412–1419.
Li, X.X., Wang, H.B., Hu, C., Yang, M., Hu, H.Y., Niu, J.F., 2015. Characteristics of biofilms and iron corrosion scales with ground and surface waters in drinking water distribution systems. Corros. Sci. 90, 331–339.
Lin, W.F., Yu, Z.S., Chen, X., Liu, R.Y., Zhang, H.X., 2013. Molecular characterization of natural biofilms from household taps with different materials: PVC, stainless steel, and cast iron in drinking water distribution system. Appl. Microbiol. Biotechnol. 97, 8393–8401.
Ma, L.P., Li, B., Jiang, X.T., Wang, Y.L., Xia, Y., Li, A.D., Zhang, T., 2017. Catalogue of antibiotic resistome and host-tracking in drinking water deciphered by a large scale survey. Microbiome 5.
Martiny, A.C., Jorgensen, T.M., Albrechtsen, H.J., Arvin, E., Molin, S., 2003. Long-term succession of structure and diversity of a biofilm formed in a model drinking water distribution system. Appl. Environ. Microbiol. 69, 6899–6907.
Perrin, Y., Bouchon, D., Delafont, V., Moulin, L., Hechard, Y., 2019. Microbiome of drinking water: a full-scale spatio-temporal study to monitor water quality in the Paris distribution system. Water Res. 149, 375–385.
Prest, E.I., Hammes, F., Kotzsch, S., van Loosdrecht, M.C.M., Vrouwenvelder, J.S., 2013. Monitoring microbiological changes in drinking water systems using a fast and reproducible flow cytometric method. Water Res. 47, 7131–7142.
Proctor, C.R., Reimann, M., Vriens, B., Hammes, F., 2018. Biofilms in shower hoses. Water Res. 131, 274–286.
Ren, H.X., Wang, W., Liu, Y., Liu, S., Lou, L.P., Cheng, D.Q., He, X.F., Zhou, X.Y., Qiu, S.D., Fu, L.S., Liu, J.Q., Hu, B.L., 2015. Pyrosequencing analysis of bacterial communities in biofilms from different pipe materials in a city drinking water distribution system of East China. Appl. Microbiol. Biotechnol. 99, 10713–10724.
Revetta, R.P., Gomez-Alvarez, V., Gerke, T.L., Curioso, C., Domingo, J.W.S., Ashbolt, N.J., 2013. Establishment and early succession of bacterial communities in monochloramine-treated drinking water biofilms. FEMS Microbiol. Ecol. 86, 404–414.
Salyers, A., Shoemaker, N.B., 2006. Reservoirs of antibiotic resistance genes. Anim. Biotechnol. 17, 137–146.
Shen, Y., Huang, C.H., Monroy, G.L., Janjaroen, D., Derlon, N., Lin, J., Espinosa-Marzal, R., Morgenroth, E., Boppart, S.A., Ashbolt, N.J., Liu, W.T., Nguyen, T.H., 2016. Response of simulated drinking water biofilm mechanical and structural properties to long-term disinfectant exposure. Environ. Sci. Technol. 50, 1779–1787.
Stanish, L.F., Hull, N.M., Robertson, C.E., Harris, J.K., Stevens, M.J., Spear, J.R., Pace, N.R., 2016. Factors influencing bacterial diversity and community composition in municipal drinking waters in the Ohio river basin, USA. PLoS One 11.
Wang, H., Masters, S., Edwards, M.A., Falkinham, J.O., Pruden, A., 2014a. Effect of disinfectant, water age, and pipe materials on bacterial and eukaryotic community structure in drinking water biofilm. Environ. Sci. Technol. 48, 1426–1435.
Wang, H., Masters, S., Hong, Y.J., Stallings, J., Falkinham, J.O., Edwards, M.A., Pruden, A., 2012a. Effect of disinfectant, water age, and pipe material on occurrence and persistence of Legionella, mycobacteria, Pseudomonas aeruginosa, and two amoebas. Environ. Sci. Technol. 46, 11566–11574.
Wang, H.B., Hu, C., Hu, X.X., Yang, M., Qu, J.H., 2012b. Effects of disinfectant and biofilm on the corrosion of cast iron pipes in a reclaimed water distribution system. Water Res. 46, 1070–1078.
Wang, H.B., Hu, C., Zhang, L.L., Li, X.X., Zhang, Y., Yang, M., 2014b. Effects of microbial redox cycling of iron on cast iron pipe corrosion in drinking water distribution systems. Water Res. 65, 362–370.
Wang, L., Zhang, J., Li, H.L., Yang, H., Peng, C., Peng, Z.S., Lu, L., 2018. Shift in the microbial community composition of surface water and sediment along an urban river. Sci. Total Environ. 627, 600–612.
Xu, L.K., Ouyang, W.Y., Qian, Y.Y., Su, C., Su, J.Q., Chen, H., 2016. High-throughput profiling of antibiotic resistance genes in drinking water treatment plants and distribution systems. Environ. Pollut. 213, 119–126.
Yu, J., Kim, D., Lee, T., 2010. Microbial diversity in biofilms on water distribution pipes of different materials. Water Sci. Technol. 61, 163–171.
Zhang, H.Y., Tian, Y.M., Kang, M.X., Chen, C., Song, Y.R., Li, H., 2019a. Effects of chlorination/chlorine dioxide disinfection on biofilm bacterial community and corrosion process in a reclaimed water distribution system. Chemosphere 215, 62–73.
Zhang, J.P., Li, W.Y., Chen, J.P., Qi, W.Q., Wang, F., Zhou, Y.Y., 2018. Impact of biofilm formation and detachment on the transmission of bacterial antibiotic resistance in drinking water distribution systems. Chemosphere 203, 368–380.
Zhang, J.P., Li, W.Y., Chen, J.P., Wang, F., Qi, W.Q., Li, Y., 2019b. Impact of disinfectant on bacterial antibiotic resistance transfer between biofilm and tap water in a simulated distribution network. Environ. Pollut. 246, 131–140.
Zhang, J.P., Li, W.Y., Wang, F., Qian, L., Xu, C., Liu, Y., Qi, W.Q., 2016. Exploring the biological stability situation of a full scale water distribution system in south China by three biological stability evaluation methods. Chemosphere 161, 43–52.
Zhang, X.J., Chen, Z., Ma, Y.P., Zhang, N., Pang, Q., Xie, X.Y., Li, Y.Z., Jia, J.P., 2019c. Response of Anammox biofilm to antibiotics in trace concentration: microbial activity, diversity and antibiotic resistance genes. J. Hazard Mater. 367, 182–187.
Zhu, Z.B., Wu, C.G., Zhong, D., Yuan, Y.X., Shan, L.L., Zhang, J., 2014. Effects of pipe materials on chlorine-resistant biofilm formation under long-term high chlorine level. Appl. Biochem. Biotechnol. 173, 1564–1578.